A meridional scan of the stratospheric gravity wave field over the ocean in 2001 (MeSSO2001)

Kaoru Sato,[1] Miho Yamamori,[2,3] Shin-Ya Ogino,[4] Noriyoshi Takahashi,[5] Yoshihiro Tomikawa,[6] and Takashi Yamanouchi[1]

Received 26 November 2002; revised 2 May 2003; accepted 13 May 2003; published 19 August 2003.

[1] In order to examine gravity wave characteristics over the ocean, we conducted a radiosonde observation campaign to scan the stratosphere meridionally over the middle Pacific with Hakuho-maru research vessel operated by the Ocean Research Institute, University of Tokyo. Seventy vertical profiles of temperature, winds, and humidity were successfully obtained over a wide latitude range of 28°N to 48°S with an interval of 1 degree. Gravity wave energy and vertical wavenumber spectra were examined as a function of latitude. Gravity wave energy is maximized in the tropical region where the convection is active and in the middle latitude region where the subtropical westerly jet is situated. The wave energy in the tropical region is greater than the climatology based on operational radiosonde observation over land regions. The gravity wave amplitude does not necessarily increase with altitude, in contradiction to simple vertical propagation. The latitudinal distribution of wave energy rather suggests that gravity waves propagate meridionally toward higher latitudes. An interesting feature is that a wave packet having large horizontal wind and temperature amplitudes is observed continuously over 7 days in the latitudinal region extending 26 degrees. Results of hodograph analysis indicate that the wave packet is due to an inertia-gravity wave with horizontal and vertical wavelengths of about 1800 km and 4–5km, respectively. This inertia-gravity wave is likely generated in association with vigorous convection in the Intertropical Convergence Zone (ITCZ) in the Northern Hemisphere and propagated southward interhemispherically. The results in this study show that there are strong nonstationary gravity wave sources over the ocean. The importance of meridionally propagating gravity waves is discussed. *INDEX TERMS:* 3314 Meteorology and Atmospheric Dynamics: Convective processes; 3334 Meteorology and Atmospheric Dynamics: Middle atmosphere dynamics (0341, 0342); 3384 Meteorology and Atmospheric Dynamics: Waves and tides; *KEYWORDS:* gravity waves, radiosondes, stratosphere, middle atmosphere dynamics, spectral analysis, convection

Citation: Sato, K., M. Yamamori, S.-Y. Ogino, N. Takahashi, Y. Tomikawa, and T. Yamanouchi, A meridional scan of the stratospheric gravity wave field over the ocean in 2001 (MeSSO2001), *J. Geophys. Res.*, *108*(D16), 4491, doi:10.1029/2002JD003219, 2003.

1. Introduction

[2] Atmospheric gravity waves are small-scale waves with the restoring force of buoyancy. They had been examined mostly from a theoretical point of view and treated as ''noise'' for weather prediction for a long time. However, it was suggested by theoretical works in 1980s that upward momentum transport by gravity waves is a key process to determine the dynamical structure of the middle atmosphere in the height region of 10–100 km such as weak wind layers around the mesopause [*Lindzen*, 1981; *Matsuno*, 1982] and in the lower stratosphere [*Tanaka and Yamanaka*, 1985] in the middle latitude region. With the aid of MST radars and radiosondes with high vertical resolution developed in the same time period, the theoretical prediction was confirmed observationally [*Tsuda et al.*, 1990; *Sato*, 1994]. Then, it is further revealed that the roles of atmospheric gravity waves are more important than expected theoretically, namely, in the summer stratosphere [*Alexander and Rosenlof*, 1996], in the equatorial stratosphere [e.g., *Sato and Dunkerton*, 1997; *Dunkerton*, 1997] and equatorial mesosphere [*Mayr et al.*, 1997]. Moreover, recent works indicate the importance of gravity waves in polar regions for the formation of polar stratospheric clouds [*Carslaw et al.*, 1998; *Shibata et al.*, 2003].

[1]National Institute of Polar Research, Tokyo, Japan.
[2]Center for Climate System Research, University of Tokyo, Tokyo, Japan.
[3]Now at Communications Research Laboratory, Tokyo, Japan.
[4]Graduate School of Science and Technology, Kobe University, Kobe, Japan.
[5]Department of Geophysics, Faculty of Science, Kyoto University, Kyoto, Japan.
[6]Research Center for Advanced Science and Technology, University of Tokyo, Tokyo, Japan.

0148-0227/03/2002JD003219$09.00

[3] One of the most dominant origins of gravity waves is topography [*Fritts and Nastrom*, 1992]. Several parameterization schemes of topographically forced gravity wave were proposed and used in the global circulation models for operational and research purposes [e.g., *McFarlane*, 1987; *Palmer et al.*, 1986; *Iwasaki et al.*, 1989]. On the other hand the parameterization of nonorographic gravity waves is needed to simulate several important features of the middle atmosphere, such as the quasi-biennial oscillation in the equatorial stratosphere and zonal wind reversal in the lower thermosphere in the middle latitude region. However, we do not have sufficient knowledge on the characteristics of nonorographic gravity waves which have a variety of sources (convection, fronts, jet stream, tropical and subtropical cyclones, etc.). Although several nonorographic gravity wave parameterizations are proposed [*Fritts and Lu*, 1993; *Medvedev and Klaassen*, 1995; *Hines*, 1997; *Alexander and Dunkerton*, 1999; *Warner and McIntyre*, 2001] so far, one of the most important issues is how the wave sources are described [e.g., *Charron et al.*, 2002].

[4] Recent atmospheric observation by satellites with GPS occultation method is powerful to examine the gravity wave distribution around the world with almost uniform quality [*Tsuda et al.*, 2000]. However, because of the low horizontal resolution, GPS observation captures only a part of gravity wave spectra. Moreover, because the observed quantities are only temperature and atmospheric density, it is difficult or impossible to estimate gravity wave parameters such as phase velocities and momentum fluxes that are necessary to quantify the gravity wave effects.

[5] As for the land regions, daily or twice daily radiosonde observations in the troposphere and lower stratosphere are made operationally at about 2000 stations for the purpose of weather forecast. The analysis of horizontal and temperature data provides the information of gravity wave propagation. *Kitamura and Hirota* [1989] and *Allen and Vincent* [1995] utilized the operational data to examine gravity wave characteristics as a function of latitude. *Yoshiki and Sato* [2000] compared the gravity wave characteristics between the Arctic and Antarctic. *Sato et al.* [1994] and *Vincent and Alexander* [2000] examined gravity waves in the tropical lower stratosphere. Now, a systematic analysis of gravity waves using original high-resolution data from operational observation is being made as a SPARC initiative [*Vincent*, 2003].

[6] On the other hand, there are little radiosonde observations over the ocean, although it occupies more than 70% of the Earth surface. As the observed wave field in land regions is sometimes masked by strong topographically-forced gravity wave events [e.g., *Sato*, 1994], it is not so easy to examine nonorographic gravity waves. Thus the observation over the ocean has a merit for investigation of nonorographic gravity waves.

[7] One approach to examine gravity waves over the ocean is the use of high-resolution global circulation model (GCM). *Sato et al.* [1999] made simulation of gravity waves using an aqua-planet GCM with horizontal and vertical resolution of T106 and 600 m, respectively. Good agreement with MST (Mesosphere-Stratosphere-Troposphere) radar observations at a middle latitude assured that the simulated gravity wave fields are realistic. Statistical characteristics of simulated gravity waves in terms of the frequency spectra as a function of latitude and the distribution of wave energy and momentum fluxes in the latitude-height section were shown. The reality over the ocean in the tropical region and high latitude region remains to be confirmed by observations.

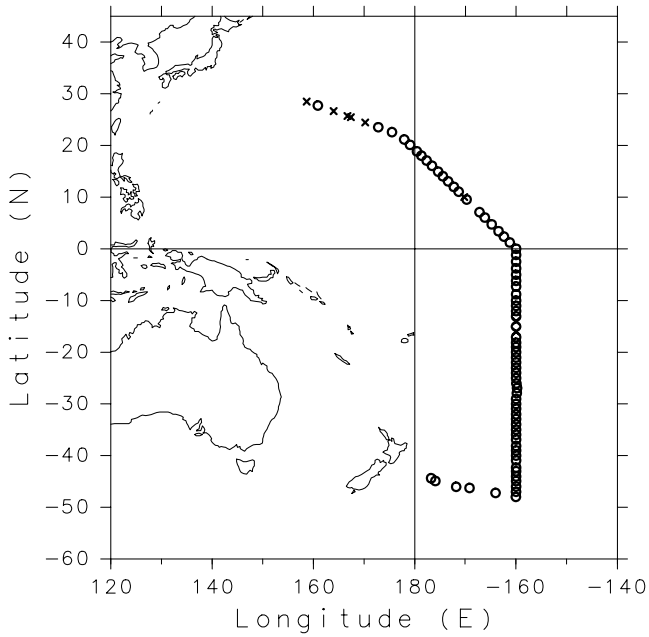

Figure 1. The locations where the GPS radiosondes were launched. The radiosondes at the locations shown by open circles (cross marks) reached (did not reach) the attitude of 24 km in the lower stratosphere.

[8] In our study we conducted a radiosonde observation campaign to scan the stratosphere meridionally over the middle Pacific with Hakuho-maru research vessel operated by the Ocean Research Institute, University of Tokyo. Seventy vertical profiles of temperature, horizontal winds, and humidity were successfully obtained covering a wide latitude range of 28°N to 48°S. Detailed description of the observation is made in section 2. A series of vertical profiles obtained by the observations is shown in section 3. Gravity wave energy and vertical wavenumber spectra are examined as a function of latitude and altitude, and compared with climatology by the SPARC Radiosonde Initiative [*Vincent*, 2003] in section 4. During the observation period an inertia-gravity wave packet is observed over 7 days propagating from the Northern Hemisphere to the Southern Hemisphere. Detailed analysis in terms of its wave parameters and source is made in section 5. Results are discussed in section 6. Summary and concluding remarks are made in section 7.

2. Observation

[9] The observation period is about one month from 27 November through 25 December 2001. To measure horizontal winds, temperature and humidity, Vaisala RS80-15GH radiosondes were launched at almost the same latitude interval of 1 degree in the latitude range of 28°N to 48°S over Hakuho-maru research vessel as shown in Figure 1. The observation points from the equator to 48°S are located along a meridian of 160°W. Although several trials were

failed in the beginning of the campaign period due to a trouble of receiving system, seventy observations in the troposphere and lower stratosphere reaching the altitude above 24 km were successfully performed. The accuracy of temperature and winds is 0.1 degree and 0.5 m s^{-1}, respectively. The wind data with original time resolution of 0.5 s by GPS observations are smoothed and recorded at every 2 s corresponding to the height resolution of about 10 m. The response time of temperature sensor is 4, 8, and 12 s at altitudes of 8, 16, and 24 km, respectively. This means that the real height resolution of the temperature data is about 20, 40, and 80 m, respectively. In this study, so as to make analysis easier, vertical profiles of temperature and winds were smoothed with a lowpass filter with a cutoff length of 100 m and interpolated at the same height intervals of 50 m.

3. Vertical Profiles of Temperature and Winds as a Function of Latitude

[10] Figures 2a, 2b and 2c are a series of temperature (T), zonal wind (u), and meridional wind (v) profiles that were obtained by the observation. The blue closed circle plotted on each profile in Figure 2a in the latitude range from 20°S to 48°S is the tropopause that is determined by the variation of vertical gradient of temperature following the definition by WMO. The red closed circle is the altitude with minimum temperature at each profile in the latitude range north of 25°S that is considered to be more appropriate tropopause definition for the tropical region than the WMO one. The tropical tropopause is located in the altitude region of 17–18 km, while the tropopause to the south of 35°S is located in the altitude region of 11–12 km. In the transition region from latitudes of 21°S to 34°S, double tropopause structure is seen, i.e., one is in the altitude region of 15–18 km as the high latitude end of the tropical tropopause and the other is in the 8–10 km region as the low latitude end of midlatitude tropopause.

[11] A strong westerly shear is observed in the lower stratosphere in the equatorial region from 10°N to 10°S (Figure 2b). The zonal wind is easterly just above the tropopause and westerly above the altitude of 23 km. This structure is similar to the observation at Singapore (1.4°N, 104.0°E) at a distance of 12,000 km (B. Naujokat, private communication, 2002) and hence considered to be associated with the quasi-biennial oscillation (QBO). The subtropical jet stream is situated in the latitude region around 30°S, which keeps thermal wind balance with the double tropopause structure seen in the temperature field. In the lower stratosphere, wind fluctuations with vertical scales of about 1 km are seen at any latitude and considered to be mostly due to gravity waves.

[12] Meridional wind shown in Figure 2c is generally weak compared with zonal wind. However, small-scale fluctuations are clearer in the meridional wind field. It is seen that the vertical wavelengths of the fluctuations are longer in the lower latitude region.

4. Gravity Wave Characteristics as a Function of Latitude

[13] In order to examine dynamical characteristics of gravity waves, we extracted perturbation from the third-order polynomial fit for a particular altitude range extending over 7 km, as fluctuation components of T', u', and v', following the SPARC gravity wave initiative.

[14] First, we calculated vertical wavenumber (m) spectra for temperature and wind fluctuations. As the spectral shape is expected to be steep, i.e., almost proportional to m^{-3} [*VanZandt*, 1982], prewhitening and recoloring processes were made before and after the spectral calculation, respectively. For temperature spectra, a correction for a finite response time of the temperature sensor was made [*Allen and Vincent*, 1995]. The response time is obtained by a linear interpolation using known values described in section 2. Obtained spectra are averaged in latitude regions extending 10 degrees with centers of 45°S, 35°S, 25°S, 15°S, 5°S, 5°N, 15°N and 25°N. Figure 3 shows the vertical wavenumber spectra of temperature, zonal and meridional wind fluctuations as a function of latitude. The slope of the spectrum proportional to m^{-3} is shown by dotted lines. It is generally seen that the spectral slope is steeper at lower latitude regions, which is clearer in temperature spectra. This feature comes mostly from the fact that smaller wavenumber components have larger spectral densities at lower latitudes. On the other hand, larger wavenumber components have spectral densities almost independent of latitudes. This tendency is seen also for zonal and meridional wind spectra.

[15] Altitude dependence of the vertical wavenumber spectra is also examined. Figure 4 shows the temperature spectra at an altitude range of 24–31 km in the middle stratosphere. The tendency of the steepness as a function of latitude is similarly observed for the middle stratosphere spectra. It is interesting that the spectral densities for the middle stratosphere are generally lower than those for the lower stratosphere in the equatorial region (5°S and 5°N).

[16] Next, we show that the gravity wave energy as a function of latitude. Kinetic energy divided by atmospheric density is defined as $\overline{u'^2 + v'^2}$ ignoring contribution of vertical wind fluctuations, and potential energy divided by density is defined as $\overline{(T'g/TN)^2}$, where N is the Brunt-Väisälä frequency calculated at each profile and g is the gravity acceleration. Figure 5 shows the result as a function of latitude for the lower and middle stratosphere. In the lower stratosphere, both kinetic and potential energy are maximized around the equator. A weak maximum is also observed for kinetic energy in the latitude region around 34°S where the subtropical westerly jet stream is situated. However, in general, the gravity wave energy is weaker at higher latitudes, which is consistent with the climatology in land regions shown by the SPARC Radiosonde Initiative [*Vincent*, 2003] and also with characteristics of gravity waves simulated by the aqua-planet GCM by *Sato et al.* [1999]. *Alexander et al.* [2002] reported a similar equatorial maximum in the potential energy using temperature data from GPS/MET satellite observations. The energy values are slightly smaller than our observation, probably partly because of coarse horizontal resolution. In the middle stratosphere the maximum of kinetic and potential energy in the tropical region is observed at off-equator in both hemispheres. The maximum around the latitude of subtropical jet stream is weak compared with that in the lower stratosphere.

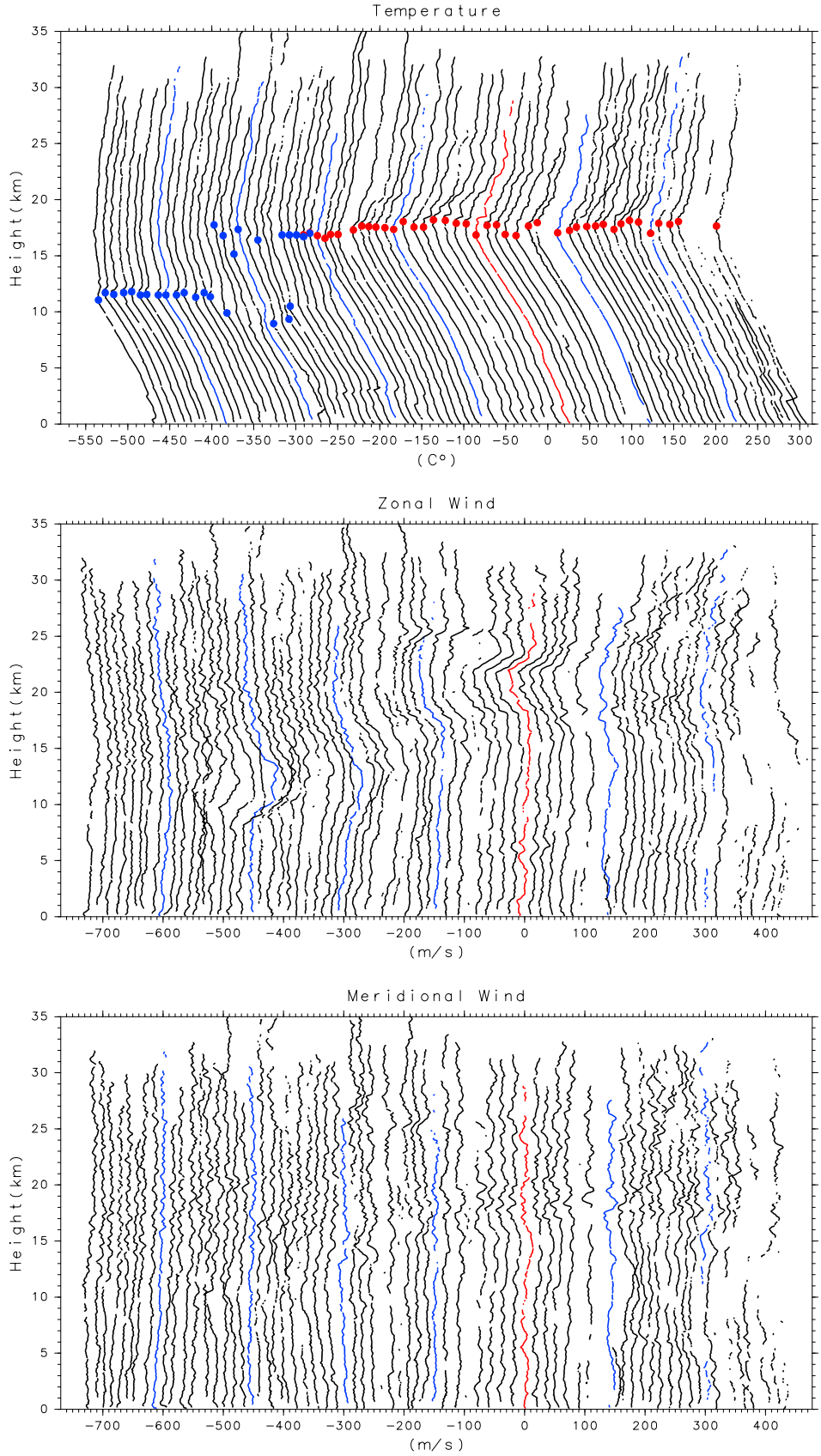

Figure 2. Series of vertical profiles of (a) temperature, (b) zonal and (c) meridional winds. Red profiles are at the equator. Blue profiles are at every 10 degree latitude. Scales on the horizontal axis are shown for the profiles of the equator. Each profile is shifted proportional to the latitude. Red and blue circles show the tropical and midlatitude tropopauses. See the text for details.

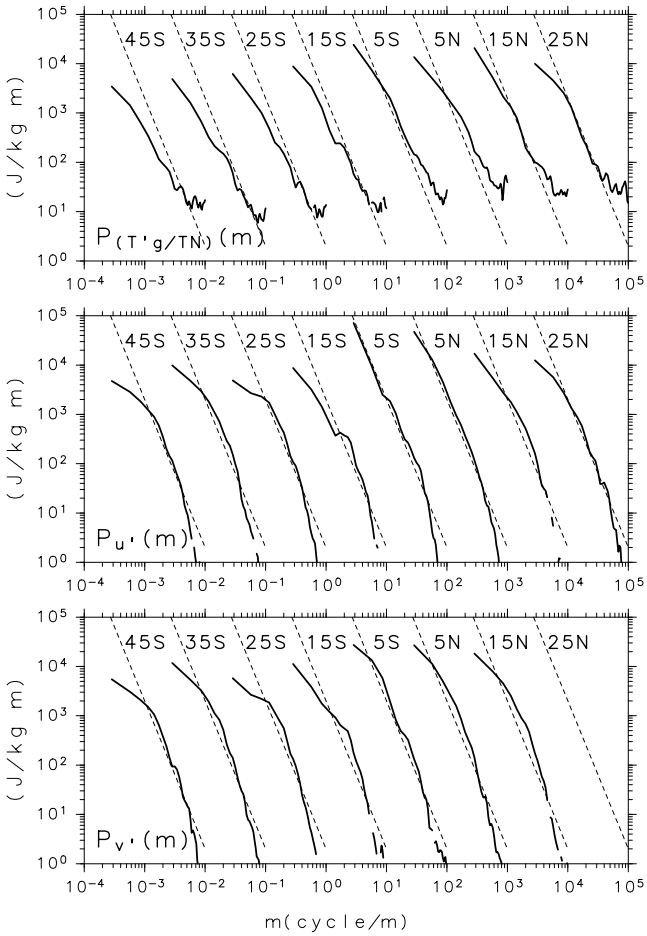

Figure 3. Vertical wavenumber spectra of temperature (T), zonal (u) and meridional (v) wind fluctuations for the altitude range of 18–25 km in the lower stratosphere as a function of latitude. Dotted lines show the slope of the spectrum proportional to m^{-3}. Scales of the horizontal axes are for the spectra for 45°S. The spectra at the other latitudes are shifted by 1 order of magnitude, respectively.

[17] It should be noted, however, that the kinetic energy maximum around the equator might be due to contamination by the QBO in the lower stratosphere. It is difficult to distinguish the QBO and embedded disturbances only from the vertical profiles. Figure 6 shows the latitude profiles of contribution to kinetic energy by zonal and meridional wind fluctuations. It is seen that the maximum around the equator is mostly contributed to by the zonal wind fluctuations, which is consistent with the above speculation. However, the distribution is not symmetric around the equator, suggesting that the peak around 4°S is due to dominant waves existing there. On the other hand, the meridional wind contribution is maximized around the latitudes of 5°S and 5°N in the lower stratosphere. In the middle stratosphere, the maxima are shifted toward higher latitude regions, i.e., around the latitudes of 15°S and 15°N. It is worth noting that the zonal wind contribution has maxima in similar latitude regions to the meridional wind maximum in the middle stratosphere. The difference in the maximum location between the lower and middle stratosphere suggests that the waves propagate toward higher latitudes from the equatorial region.

5. Interhemispheric Propagation of an Inertia-Gravity Wave

[18] Since the radiosonde observation was made 4 to 5 times daily and the ship did not move at constant speed, we need to be careful to interpret the phase structure seen in the meridional cross section made from the observation data. However, we could detect a systematic structure in this observation.

[19] Figure 7a shows the meridional cross section of the meridional wind which is smoothed in the vertical and in the latitudinal with lowpass filters with cutoff lengths of 2 km and 5 degrees (roughly corresponding to the running mean of 1 km and 2 degrees), respectively. Several phase lines tilted northward and upward are seen in the stratosphere in the latitude region of 25°S to 10°N. Moreover, the regions with large amplitudes are located at higher altitudes at more southern latitudes (as shown by a thick broken arrow. Details are described later in this section). These features may be due to upward propagation of a gravity wave packet.

[20] Figure 8 shows a contour map of the logarithm of the Brunt-Väisälä frequency squared, obtained from radiosonde temperature data, which is a measure of static stability of the atmosphere. Red and blue closed circles show the tropical and midlatitude tropopauses, respectively, as in Figure 2a. Roughly speaking, the static stability is high in the tropical lower stratosphere and low below the tropopause at any latitudes. A characteristic structure with high static stability associated with low static stability above is seen in the lower troposphere ($z = 2 - 5$ km) in the latitude regions around 25 degrees in both hemispheres, corresponding to an inversion layer possibly due to large-scale subsidence of the atmosphere in the subtropical region.

[21] The Brunt-Väisälä frequency squared is also a convenient quantity to see small-scale vertical structure of temperature, because it is proportional to the vertical gradient of temperature. It is important that a wave-packet like structure observed in Figure 7 is also seen in Figure 8 in the tropical stratosphere.

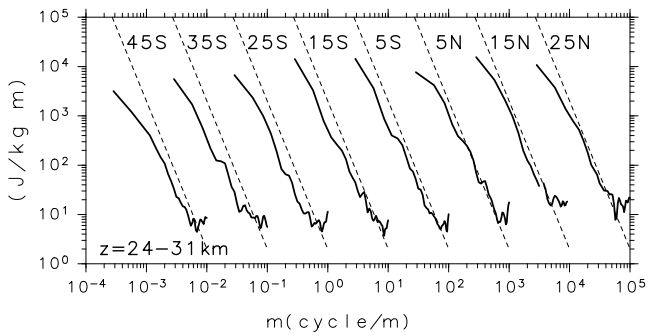

Figure 4. The same as Figure 3a but for temperature fluctuations in the altitude range of 24–31 km in the middle stratosphere.

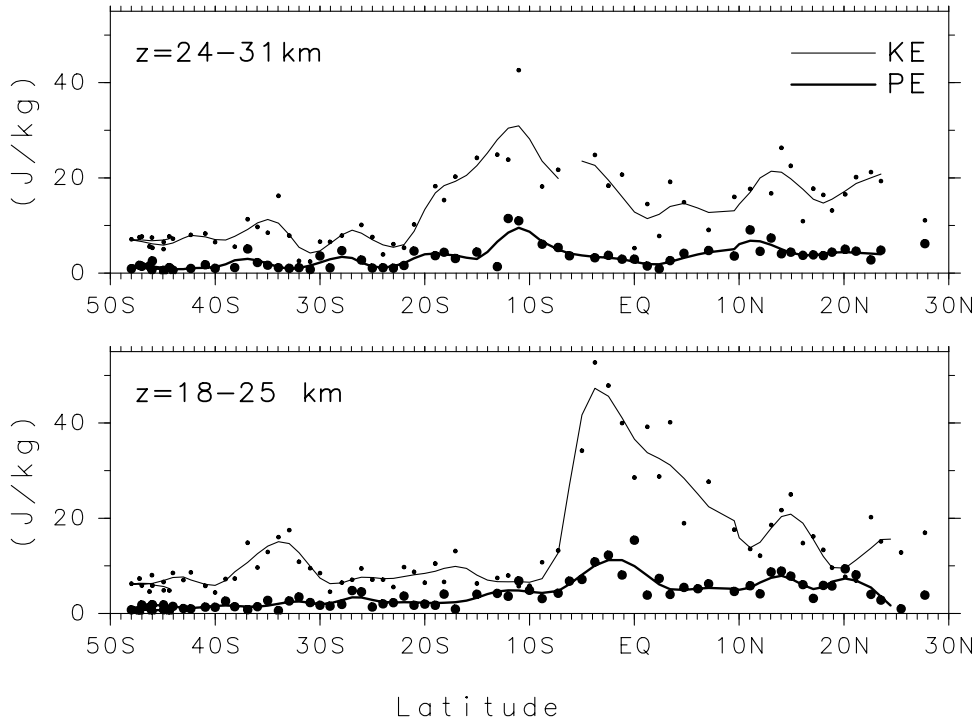

Figure 5. Gravity wave energy divided by atmospheric density as a function of latitude for (a) the middle (an altitude range of 24–31 km) and (b) lower stratosphere (18–25 km). Large and small closed circles show potential and kinetic energy obtained at each latitude, respectively. Thin and thick curves show smoothed profiles for kinetic and potential energy by using a lowpass filter with a cutoff length of 6 degrees, respectively.

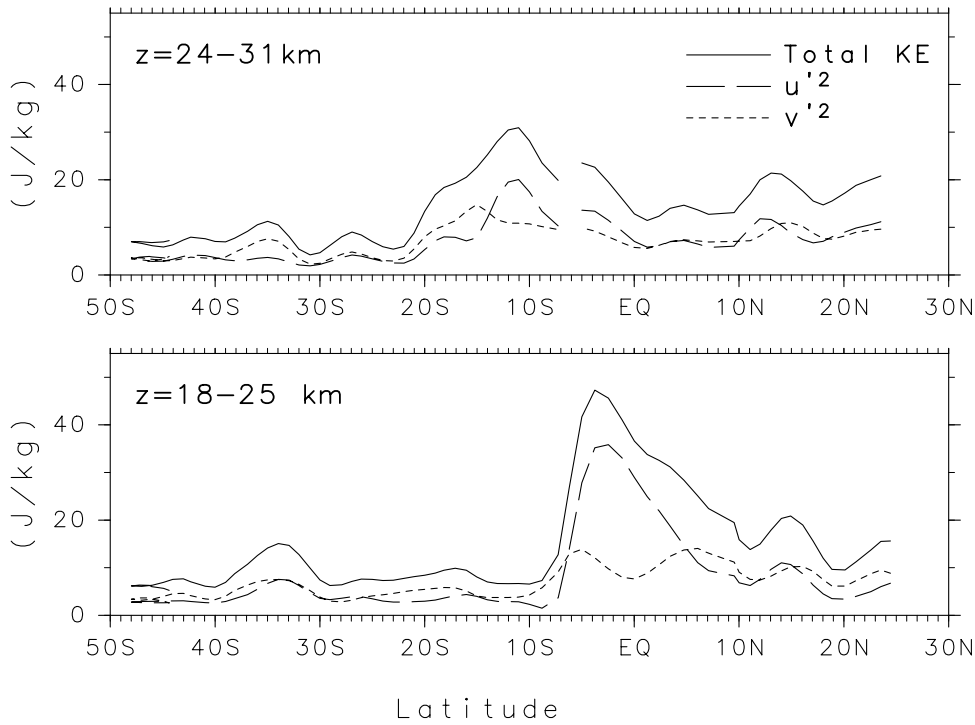

Figure 6. The same as Figure 5 but for total kinetic energy (solid curves) and contribution to kinetic energy by zonal (dashed curves) and meridional (dotted curves) wind fluctuations.

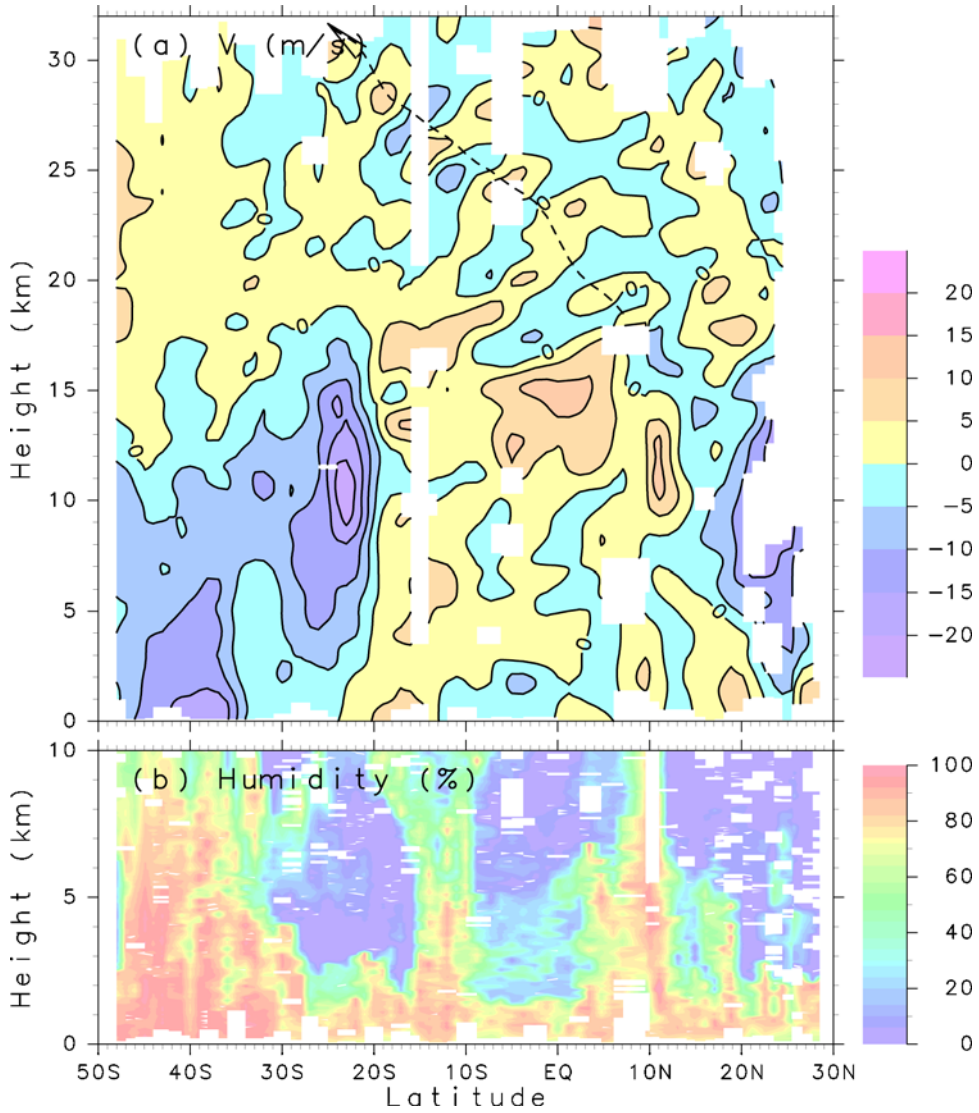

Figure 7. A meridional cross section of meridional winds (a) and humidity (b) over the middle Pacific observed by radiosondes in 30 November to 25 December 2002. Contour intervals are 5 m s^{-1} for meridional winds. A dashed arrow indicates the propagation of the inertia-gravity wave packet.

[22] Thus we will make further analysis to confirm this speculation that the phase structure observed in the meridional-cross section is due to an inertia-gravity wave. First, we focus on the latitude region of 11°S to 19°S where the wave structure is clear in the height region of 23–32 km. In this region the cruise speed was almost constant (about 550 km d^{-1}). Vertical profiles of zonal and meridional wind fluctuations are shown in Figure 9. Horizontal spacing of the profiles is proportional to the time difference of observation. As shown by a dotted line, systematic downward phase propagation is seen. The vertical phase speed observed on the ship c_{obsz} is estimated at about −1.6 km d^{-1}. On the other hand, the fluctuations show a packet-like structure as shown by a thick vertical line on the right at each profile. A solid arrow shows the upward propagation of the wave packet. The upward packet speed, i.e., vertical group velocity observed on the ship c_{gobsz} is estimated at about 1.5 km d^{-1}.

[23] Next, wave parameters are estimated from vertical profiles of wind and temperature fluctuations for each radiosonde observation. The fluctuations of T', u', and v' are fitted into sinusoidal waves under the restriction of the inertia-gravity wave theory that T' takes its maximum at the height where the horizontal wind speed $\sqrt{(u'^2 + v'^2)}$ takes its minimum.

[24] The vertical wavenumber m is directly estimated from the fitting. The direction of hodograph rotation with height indicates vertical energy propagation. Clockwise (anticlockwise) rotation with height means upward (downward) energy propagation in the Northern Hemisphere. This relation is opposite in the Southern Hemisphere. The horizontal wavenumber vector direction, i.e., horizontal phase velocity direction is estimated as that of the long axis of hodograph, although an ambiguity of 180 degrees remains. This ambiguity is fixed from the phase relation with the temperature fluctuation. Next the intrinsic frequency $\hat{\omega}$ is

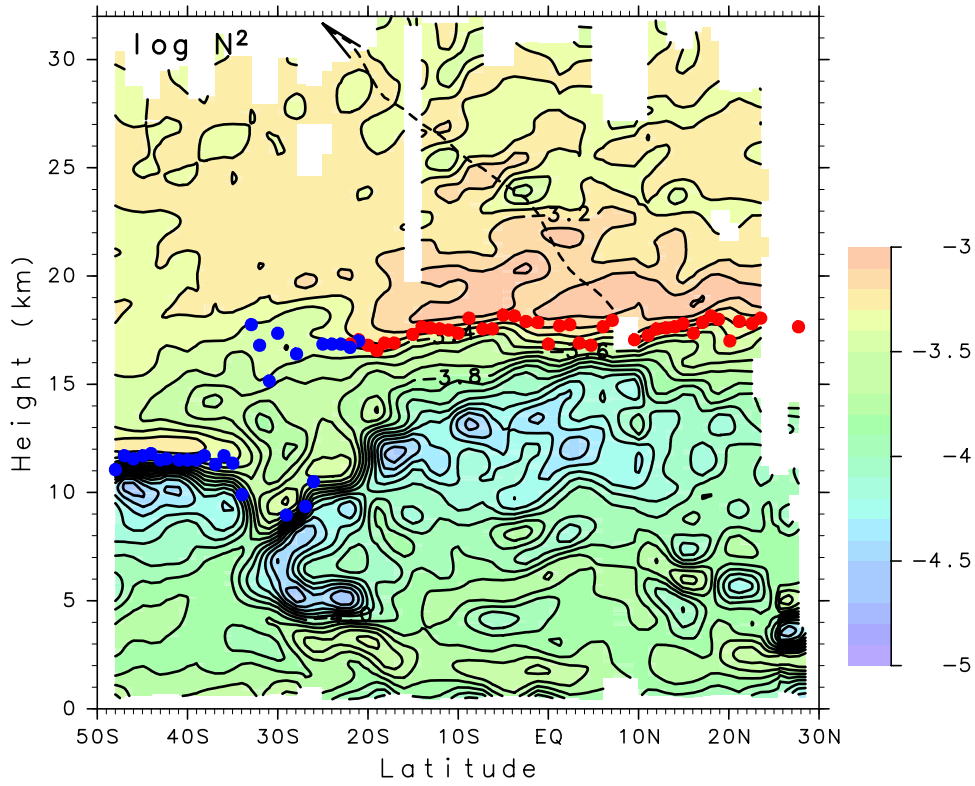

Figure 8. The same as Figure 7 but for logarithm of the Brunt-Väisälä frequency squared. Contour intervals are 0.1. Red and blue closed circles indicate the tropical and midlatitude tropopauses, respectively.

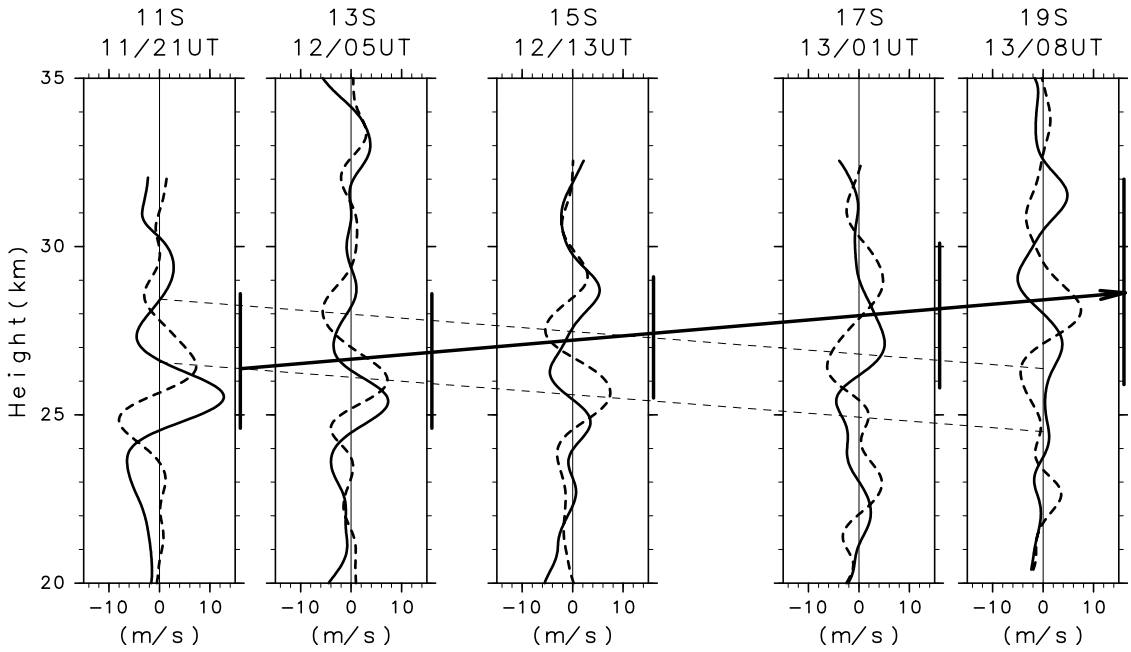

Figure 9. Vertical profiles of zonal (solid curves) and meridional (dashed curves) wind fluctuations at latitudes of 11°S, 13°S, 15°S, 17°S, and 19°S. Thin dashed lines and a thick arrow show the vertical phase and energy propagation, respectively. The horizontal spacing between the profiles is proportional to the observation time difference.

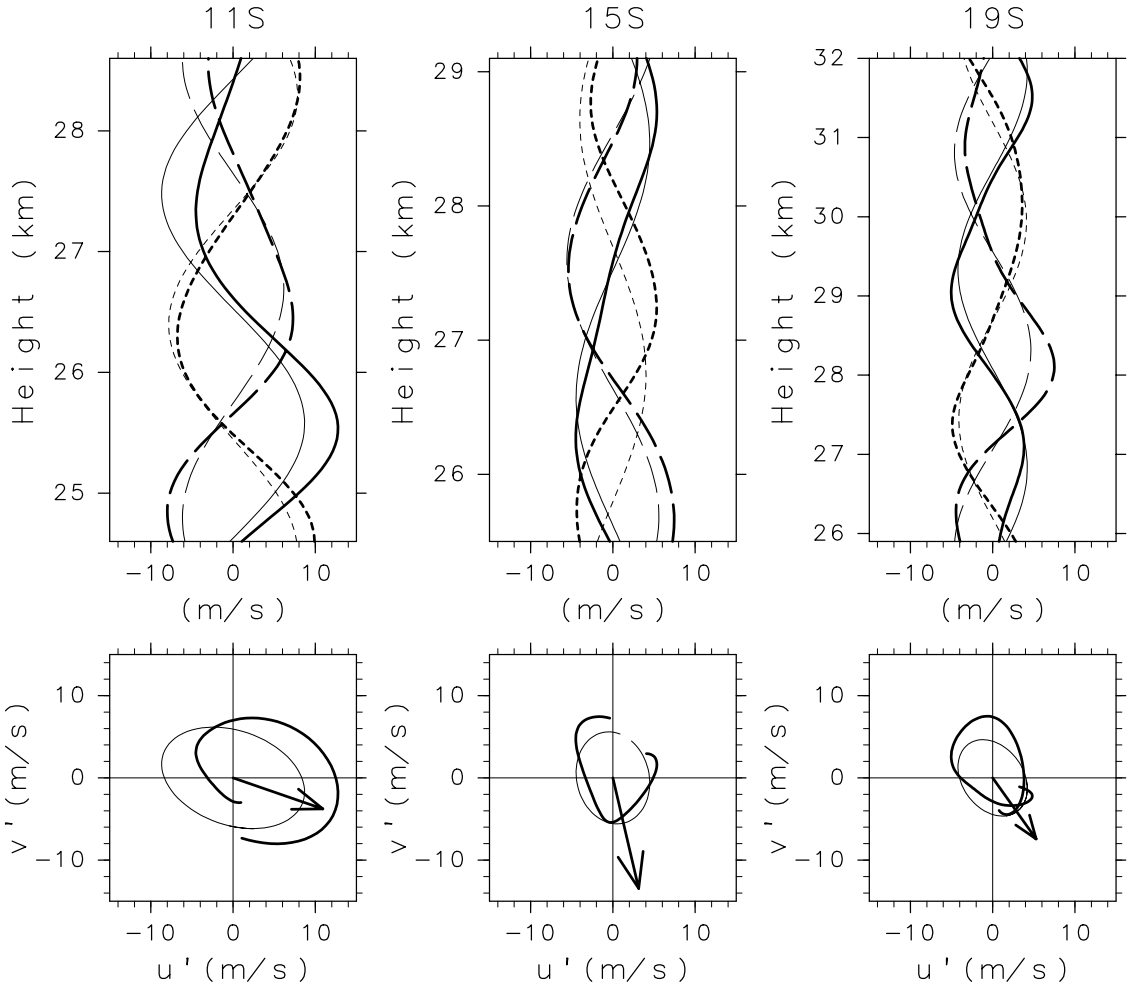

Figure 10. Top panels show vertical profiles of zonal (thick solid curves) and meridional (thick long-dashed) wind and temperature fluctuations (thick short-dashed) and respective fitted curves (thin solid, long-dashed, and short-dashed) in the altitude region in which the fitting was successfully made at latitudes of 11°S, 15°S, and 19°S. Temperature fluctuations were plotted as the value of $T'g/TN$. Observed hodographs (thick curves) and fitted curves (thin curves) are shown in the bottom panels. Arrows show the ground-based phase velocities estimated by the hodograph analysis.

estimated from the ratio of long (a) to short (b) axes of the hodograph in the following:

$$\frac{f}{\hat{\omega}} = \frac{b}{a}, \tag{1}$$

where f is the inertial frequency. Moreover, using the dispersion relation of an inertia-gravity wave

$$\frac{\hat{\omega}^2 - f^2}{N^2 - \hat{\omega}^2} = \frac{k^2}{m^2} \tag{2}$$

horizontal wavenumber k can be estimated. From these calculations we can estimate three dimensional wavenumber vector and intrinsic frequency.

[25] The validity of the estimation can be confirmed by theoretical consistency of horizontal wind and temperature fluctuation amplitudes. Note that for the wave parameter estimation described above, only phase relation between horizontal wind and temperature fluctuations was used and amplitudes were not. The temperature fluctuation amplitude can be estimated from wind fluctuation amplitude a using a theoretical polarization relation of the inertia-gravity wave as well as estimated wave parameters;

$$T_{\text{amp est}} = \frac{Nk}{m\hat{\omega}} \frac{NT}{g} a. \tag{3}$$

Thus the coincidence of $T_{\text{amp est}}$ and observed amplitude of temperature fluctuation $T_{\text{amp obs}}$ means that the assumption of inertia-gravity wave is valid and that the wave parameters are accurately estimated.

[26] The wave parameter estimation was made for five profiles at latitudes of 11°S, 13°S, 15°S, 17°S and 19°S with few missing data points. Meaningful wave parameters could be estimated for the profiles of 11°S, 15°S and 19°S. Fitted profiles and hodographs are shown in Figure 10. Estimated wave parameters are summarized in Table 1. Note that the estimated and observed temperature fluctuation amplitudes accord well. The failure of estimation for

Table 1. Wave Parameters Obtained by Hodograph Analysis at Latitudes of 11°S, 15°S, and 17°S[a]

Lat.	Dir. of wave vector, deg	λ_h, km	λ_z, km	τ, h	c_h, m s^{-1}	c_{gy}, km d^{-1}	c_{gz}, km d^{-1}	a, m s^{-1}	$T'_{amp\ obs}$, K	$T'_{amp\ est}$, K
11°S	19 (ESE)	1700	3.8	41	12	210	1.3	9.0	2.4	2.7
15°S	76 (SSE)	1900	3.8	38	14	490	1.0	5.7	1.2	1.4
19°S	54 (SE)	1700	5.0	52	9	560	2.0	5.1	1.2	1.4
Ave.	49 (SE)	1800	4.2	44	12	420	1.4	6.6	1.6	1.8

[a]Direction of the wave vector is taken clockwise from the east. λ_h is horizontal wavelength, λ_z is vertical wavelength, τ is ground-based wave period, c_h is horizontal phase velocity, c_{gy} is ground-based southward group velocity, c_{gz} is upward group velocity, a is amplitude of horizontal wind component in the direction of wave vector, $T'_{amp\ obs}$ is observed amplitude of temperature component, $T'_{amp\ est}$ is amplitude of temperature component estimated from v_{amp} and wave parameters.

the other profiles is probably due to contamination of the other disturbances.

[27] An important point is that the estimated wave parameters for 11°S, 15°S and 19°S are similar. The horizontal and vertical wavelengths are about 1800 km and 4.2 km, respectively. The horizontal phase propagation is southeastward. The vertical energy propagation is upward. This means that the fluctuations observed in the latitude region of 11°S–19°S are due to the same wave event.

[28] In order to confirm the accuracy of the wave parameter estimation further, the estimated vertical phase and vertical group velocities are compared with observation in Figure 9. Figure 11 shows schematic structure of the inertia-gravity wave. Taking a horizontal phase velocity direction of 49 degrees clockwise from the east and a horizontal wavelength of 1800 km, the meridional wavelength is estimated at 2300 km (Figure 11a). Figure 11b shows the meridional-cross section of the phase structure of the inertia-gravity wave. The vertical wavelength of 4.2 km was taken.

[29] Since the cruise speed was 550 km d^{-1}, the nominal vertical phase speed (i.e., vertical phase speed observed on the ship) assuming that the wave structure is stationary (i.e., ground-based phase speed is zero) is about +1.0 km d^{-1}. On the other hand, the ground-based vertical phase speed (λ_z/τ) estimated by the hodograph analysis is about −2.3 km d^{-1}. Thus the vertical phase speed relative to the ship is estimated at −1.3 km d^{-1}. This value is almost comparable to the observation c_{obsz} of −1.6 km d^{-1}.

[30] The vertical group velocity relative to the ship is estimated at +1.4 km d^{-1} from the hodograph analysis. This almost accords well with the observed vertical group velocity c_{gobsz} of +1.5 km d^{-1}.

[31] Moreover, the consistency of horizontal group velocity is confirmed. In order to observe the same wave packet for a long time as in this case, the cruise speed should be comparable to the horizontal group velocity of waves. Assuming that the background meridional wind is zero (see Figure 7), the horizontal group velocity estimated from the hodograph analysis is about 420 km d^{-1}. This value is considered consistent with the cruise speed of about 550 km d^{-1} because the ambiguity of the background meridional wind (i.e., that of meridional group velocity estimation) in the current discussion can be 1–2 m s^{-1}, namely, 90–170 km d^{-1}.

[32] The consistency of the vertical phase speed, vertical and meridional group velocities shown above assures the inference that the wave structure observed in the latitude region of 11°S–19°S is due to the same inertia-gravity wave.

[33] The gravity wave sources are usually considered to be in the troposphere, although there are some exceptions such as the polar-night jet in the stratosphere [*Sato*, 2000]. Assuming that the vertical group velocity of 1.5 km d^{-1} is constant during the wave propagation, we estimated roughly the vertical location of the inertia-gravity wave packet observed in the latitude region of 11°S–19°S and the time when the wave packet was situated at the tropopause (about 18 km). The calculation was made forward and backward with a start point of the 27.5 km altitude and 19° latitude (see Figure 9). A thick dashed arrow in Figure 7 shows the propagation of the wave packet. Note that as the time

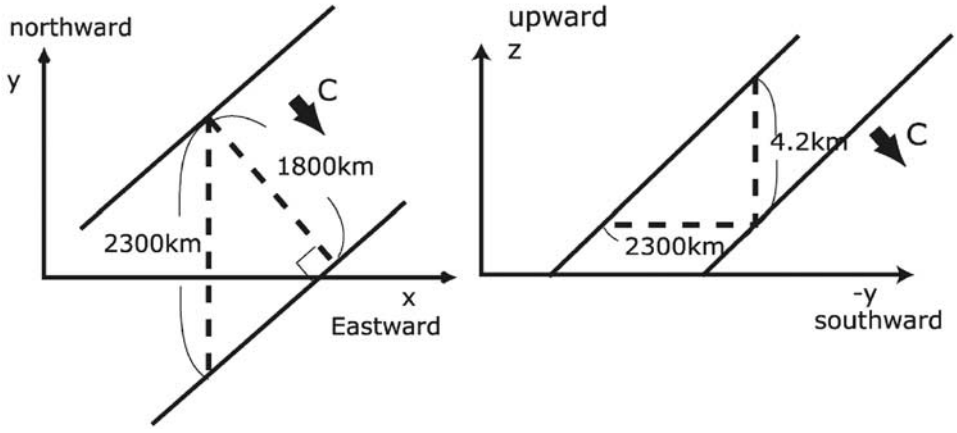

Figure 11. A schematic illustration of the inertia-gravity wave structure detected by observation. (a) Horizontal phase structure. (b) Meridional cross section of the phase structure.

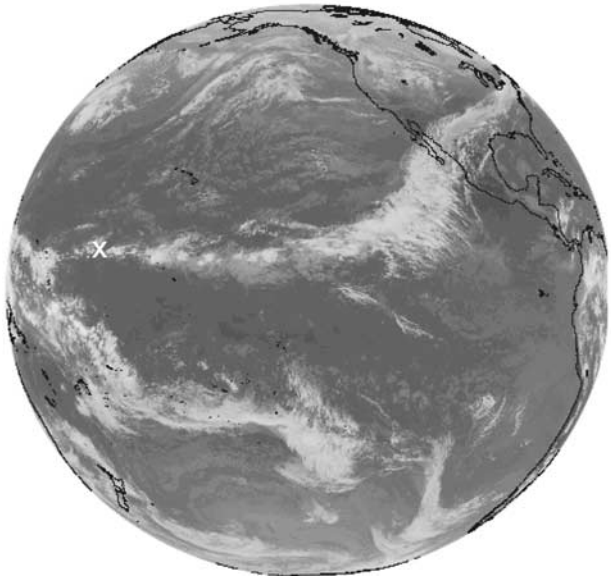

Figure 12. An IR picture of a geostationary satellite of GOES-W at 2100 UT of 6 December 2001 when the wave packet was located around the tropopause. The ship location is shown by a cross mark.

difference between observations at adjacent latitudes is not constant, the ray is not a simple straight line in the meridional cross section. The continuous wavy structure consistent with the estimated group velocity is observed in the latitude range from 8°N to 25°S in the height range of 18–31 km, indicating that this particular wave packet was observed over 7 days. The wave packet was situated at the tropopause (around 18 km) at 0700 UT of 6 December 2001 when the ship was located at the latitude of 8°N.

[34] Figure 12 shows an IR picture of a geostationary satellite of GOES-W at 2100 UT of 6 December 2001 when the wave packet was located around the tropopause. The location of the ship at this time is shown by a cross mark. A zonally elongated cloud band is observed around the latitude of 8°N where the ship was located. This cloud band corresponds to the Northern Hemisphere Intertropical Convergence Zone (ITCZ). Thus it is likely that the inertia-gravity wave packet detected by this cruise observation was excited by convection in ITCZ. In fact, when the ship was located around 8°N, the weather was stormy and a few balloon launches were failed under this condition. The convective activity is suggested by the observation of high humidity extending to the upper troposphere around 8°N seen in Figure 7b.

6. Discussion

6.1. Height Dependence of the Vertical Wavenumber Spectra

[35] As shown by many observational papers using MST radars and radiosondes with fine vertical resolution, it was known that the horizontal wind and temperature fluctuations have vertical wavenumber spectra with a characteristic shape of m^{-3} at their higher wavenumber end (O(1/1 km) to O(1/100 m)) [*VanZandt*, 1982; *Tsuda et al.*, 1989; *Tsuda et al.*, 1991; *Sato*, 1993, 1994]. Previous theories on vertical wavenumber spectra in terms of gravity waves mostly consider the vertical propagation [e.g., *Smith et al.*, 1987; *Sato and Yamada*, 1994]. Although the wave structure is modified by the large-scale wind and atmospheric stability variation, the gravity wave amplitude basically increases exponentially as the altitude increases when dissipation processes can be ignored, since the air density decreases exponentially. On the other hand, the gravity wave amplitude is limited, in other words, saturated by dissipation processes such as local convective/dynamical instability and radiation. By taking the gravity wave saturation into account, some aspects such as the vertical change of characteristic wavenumber, i.e., the smallest wavenumber of the spectral range having a shape of m^{-3} [*Murayama et al.*, 1992] can be explained.

[36] However, the gravity waves can propagate horizontally as shown by present study. Thus the altitude dependence of the gravity wave spectra needs to be explained including this effect. An interesting feature of the wavenumber spectra observed by our experiment is that the spectrum at 5°S has smaller amplitude at the higher altitude range. This feature seems inconsistent with exponential growth of gravity wave amplitudes in the vertical at a glance.

[37] The inertia-gravity wave discussed in section 5 is dominant around the latitude of 5°S in the lower altitude region of 18–25 km for which the spectra were calculated, whereas it is dominant around 15°S in the higher region of 24–31 km. This explains the feature that the gravity wave energy is maximized in the higher latitude region at the higher altitude region in Figure 5. The vertical wavelength of the inertia-gravity wave of 4–5 km corresponds to the smallest wavenumber shown in the spectra (Figure 4). Thus the smaller amplitude at higher altitude region at 5°S is likely due to the escape of this inertia-gravity wave to the higher latitude region. This inference is consistent with the fact that the spectral amplitude at the smallest wavenumber is larger at higher altitude region at 15°S.

6.2. Importance of the Meridionally Propagating Gravity Waves

[38] It is widely recognized that gravity waves excited in the lower atmosphere propagate upward and deposit the zonal momentum in the middle and upper atmosphere. The thermal structure largely apart from the radiative balance that is observed in the lower stratosphere and the upper mesosphere is explained partly and mainly, respectively, by the existence of meridional circulation due to the gravity wave-induced force. The gravity waves propagating purely meridionally do not associate with vertical flux of zonal momentum, so their importance tends to be ignored. However, it is considered that meridionally propagating gravity waves have their own roles for the momentum balance in the middle atmosphere.

[39] First, if the wavenumber vector has nonzero zonal component, the gravity wave propagates vertical flux of zonal momentum meridionally. It means that the zonal momentum exchange occurs between different latitudes. *Sato et al.* [1999] analyzed vertical flux of zonal and meridional momentum in the meridional cross section using high-resolution GCM simulation of gravity waves, and showed meridional propagation of gravity waves with

associated significant vertical flux of zonal momentum. In particular, gravity waves excited by convection in the tropical region seem important because they associate with large momentum fluxes. They propagate energy upward and poleward and can reach the polar region above the middle stratosphere as discussed by the ray tracing calculations by *Sato* [2000].

[40] Second, several recent studies using satellite observation data [*Lieberman*, 1999] and using a GCM [*Miyahara et al.*, 2000] showed that the vertical flux of meridional momentum itself is important in the mesosphere and lower thermosphere. As described by *Andrews et al.* [1987], it has been considered that the zonal mean zonal wind and geopotential height fields are in the gradient-wind balance and the departure from the balance is small. However, this is not the fact in the mesosphere and lower thermospheric region. *Lieberman* [1999] and *Miyahara et al.* [2000] discussed that the departure from the gradient-wind balance is possibly due to the dissipation of tides and gravity waves with associated vertical flux of meridional momentum.

7. Summary and Concluding Remarks

[41] In order to examine gravity wave characteristics over the ocean, we conducted a radiosonde observation campaign to scan the stratosphere meridionally over the middle Pacific with Hakuho-maru research vessel operated by the Ocean Research Institute, University of Tokyo. Seventy vertical profiles of temperature, winds, and humidity were successfully obtained over a wide latitude range of 28°N to 48°S with almost the same latitudinal interval of 1 degree.

[42] Gravity wave energy and vertical wavenumber spectra were examined as a function of latitude. Gravity wave energy is maximized in the tropical region where the convection is active and in the middle latitude region where the subtropical westerly jet is situated. The wave energy in the tropical region is greater than the climatology based on operational radiosonde observation over land regions shown by the SPARC Radiosonde Initiative [*Vincent*, 2003], while it is comparable in the higher latitude region. The results in this study indicate that there are strong non-stationary gravity wave sources over the ocean. The importance of meridionally propagating gravity waves was discussed. It was also shown that the vertical wavenumber spectra of horizontal wind and temperature fluctuations have slope steeper at lower latitudes. The gravity wave amplitude does not simply increase with altitude, in contradiction to simple vertical propagation. The latitudinal distribution of wave energy rather suggests that gravity waves propagate meridionally from the tropical regions toward higher latitudes.

[43] An interesting feature is that a wave packet having large horizontal wind and temperature amplitudes of 6–9 m s^{-1} and 1.5–2.5 K is observed continuously over 7 days in the latitudinal region extending 26 degrees. Results of hodograph analysis indicate that the wave packet can be explained by an inertia-gravity wave with a horizontal wavelength of about 1800 km and a vertical wavelength of 4–5 km. This inertia-gravity wave is likely generated in association with vigorous convection in the Intertropical Convergence Zone (ITCZ) in the Northern Hemisphere and propagated southward interhemispherically. It was seen that this inertia-gravity wave contributes largely to the shape of the vertical wavenumber spectra and latitudinal distribution of gravity wave energy.

[44] Further analysis of gravity wave characteristics in the middle latitude region based on this experiment will be presented elsewhere. The data obtained in our radiosonde observation is useful for the validation of satellite temperature data in the ocean obtained by the GPS occultation method. In our campaign observation, we could detect an interesting phenomenon of interhemispheric propagation of gravity waves excited by tropical convection. In order to examine the generality or uniqueness of such a phenomenon, accumulation of similar observations over the ocean is important, because characteristics of the gravity wave sources over the ocean such as convection, cyclones, and jet streams depend on season and geophysical region.

[45] **Acknowledgments.** The authors thank R. Kimura, H. Niino, K. Ishikawa and their students at Ocean Research Institute (ORI), University of Tokyo, Japan, for their heartfelt support to perform this experiment. They are also indebted to I. Koike and M. Terazaki at ORI, PIs of the Hakuho-maru research cruise for their giving us an opportunity of this experiment. K. Hara at National Institute of Polar Research (NIPR), Japan, helped the launch of radiosondes during the cruise. Thanks are also for G. Hashida and N. Hirasawa at NIPR, H. Nakamura and N. Yoshizaki at Meteorological Research Institute, Japan, F. Kobayashi at National Defense Academy, Japan for their kind help during the preparation stage of our experiment. The IR Satellite picture is provided by Space Science and Engineering Center, University of Wisconsin-Madison and National Oceanic and Atmospheric Administration, USA. This research was supported by Grant-in-Aid for Scientific Research (B)(2) 12440126 of the Ministry of Education, Culture, Sports, Science and Technology, Japan.

References

Alexander, M. J., and T. J. Dunkerton, A spectral parameterization of mean-flow forcing due to breaking gravity waves, *J. Atmos. Sci.*, *56*, 4167–4182, 1999.

Alexander, M. J., and K. H. Rosenlof, Nonstationary gravity wave forcing of the stratospheric zonal mean wind, *J. Geophys. Res.*, *101*, 23,465–23,474, 1996.

Alexander, M. J., T. Tsuda, and R. A. Vincent, Latitudinal variations observed in gravity waves with short vertical wavelengths, *J. Atmos. Sci.*, *59*, 1394–1404, 2002.

Allen, S. J., and R. A. Vincent, Gravity wave activity in the lower atmosphere: Seasonal and latitudinal variations, *J. Geophys. Res.*, *100*, 1327–1350, 1995.

Andrews, D. G., J. R. Holton, and C. B. Leovy, *Middle Atmosphere Dynamics*, 489 pp., Academic, San Diego, Calif., 1987.

Carslaw, K. S., et al., Increased stratospheric ozone depletion due to mountain-induced atmospheric waves, *Nature*, *391*, 675–678, 1998.

Charron, M., E. Manzini, and C. D. Warner, Intercomparison of gravity wave parameterizations: Hines Doppler-spread and Warner and McIntyre ultra-simple schemes, *J. Meteorol. Soc. Jpn.*, *80*, 335–345, 2002.

Dunkerton, T. J., The role of gravity waves in the quasi-biennial oscillation, *J. Geophys. Res.*, *102*, 26,053–26,076, 1997.

Fritts, D. C., and W. M. Lu, Spectral estimates of gravity wave energy and momentum fluxes, II. Parameterization of wave forcing and variability, *J. Atmos. Sci.*, *50*, 3695–3713, 1993.

Fritts, D. C., and G. D. Nastrom, Sources of mesoscale variability of gravity waves. part II: Frontal, convective and jet stream excitation, *J. Atmos. Sci.*, *49*, 111–127, 1992.

Hines, C. O., Doppler-spread parameterization of gravity-wave momentum deposition in the middle atmosphere. 1. Basic formulation, *J. Atmos. Sol. Terr. Phys.*, *59*, 371–386, 1997.

Iwasaki, T., S. Yamada, and K. Tada, A parameterization scheme of orographic gravity wave drag with two different vertical partitionings part I: Impacts on Medium-range forecasts, *J. Meteorol. Soc. Jpn.*, *67*, 11–27, 1989.

Kitamura, Y., and I. Hirota, Small-scale disturbances in the lower stratosphere revealed by daily rawin sonde observations, *J. Meteorol. Soc. Jpn.*, *67*, 817–831, 1989.

Lieberman, R. S., The gradient wind in the mesosphere and lower thermosphere, *Earth Planet. Space*, *51*, 751–761, 1999.

Lindzen, R. S., Turbulence and stress due to gravity wave and tidal breakdown, *J. Geophys. Res.*, *86*, 9707–9714, 1981.

Matsuno, T., A quasi one-dimensional model of the middle atmosphere circulation interacting with internal gravity-waves, *J. Meteorol. Soc. Jpn.*, *60*, 215–226, 1982.

Mayr, H. G., J. G. Mengel, C. O. Hines, K. L. Chan, N. F. Arnold, C. A. Reddy, and H. S. Porter, The gravity wave Doppler spread theory applied in a numerical spectral model of the middle atmosphere: 2. Equatorial oscillations, *J. Geophys. Res.*, *102*, 26,093–26,105, 1997.

McFarlane, N. A., The effect of orographically excited gravity wave drag on the general circulation of the lower stratosphere and troposphere, *J. Atmos. Sci.*, *44*, 1775–1880, 1987.

Medvedev, A. S., and G. P. Klaassen, Vertical evolution of gravity wave spectra and the parameterization of associated wave drag, *J. Geophys. Res.*, *100*, 25,841–25,853, 1995.

Miyahara, S., D. Yamamoto, and Y. Miyoshi, On the geostrophic balance of mean zonal winds in the Mesosphere and lower Thermosphere, *J. Meteorol. Soc. Jpn.*, *78*, 683–688, 2000.

Murayama, Y., T. Tsuda, M. Yamamoto, T. Nakamura, T. Sato, S. Kato, and S. Fukao, Dominant vertical scales of gravity waves in the middle atmosphere observed with the MU radar and rocketsondes, *J. Atmos. Terr. Phys.*, *54*, 339–346, 1992.

Palmer, T. N., G. J. Shutts, and R. Swinbank, Alleviation of a systematic westerly bias in general circulation and numerical weather prediction models through an orographic gravity wave drag parameterization, *Q. J. R. Meteorol. Soc.*, *112*, 1001–1040, 1986.

Sato, K., Small-scale wind disturbances observed by the MU radar during the passage of Typhoon Kelly, *J. Atmos. Sci.*, *50*, 518–537, 1993.

Sato, K., A statistical study of the structure, saturation and sources of inertio-gravity waves in the lower stratosphere observed with the MU radar, *J. Atmos. Terr. Phys.*, *56*, 755–774, 1994.

Sato, K., Sources of gravity waves in the polar middle atmosphere, *Adv. Polar Upper Atmos. Res.*, *14*, 233–240, 2000.

Sato, K., and T. J. Dunkerton, Estimates of momentum flux associated with equatorial Kelvin and gravity waves, *J. Geophys. Res.*, *102*, 26,247–26,261, 1997.

Sato, K., and M. Yamada, Vertical structure of atmospheric gravity waves revealed by the wavelet analysis, *J. Geophys. Res.*, *99*, 20,623–20,631, 1994.

Sato, K., F. Hasegawa, and I. Hirota, Short-period disturbances in the equatorial lower stratosphere, *J. Meteorol. Soc. Jpn.*, *72*, 423–432, 1994.

Sato, K., T. Kumakura, and M. Takahashi, Gravity waves observed in a high-resolution GCM simulation, *J. Atmos. Sci.*, *56*, 1005–1018, 1999.

Shibata, T., K. Sato, H. Kobayashi, M. Yabuki, and M. Shiobara, The Antarctic polar stratospheric clouds under the temperature perturbation by non-orographic inertia gravity waves observed by micro pulse lidar at Syowa station, *J. Geophys. Res.*, *108*(D3), 4105, doi:10.1029/2002JD002713, 2003.

Smith, S. A., D. C. Fritts, and T. E. VanZandt, Evidence of a saturation spectrum of atmospheric gravity waves, *J. Atmos. Sci.*, *44*, 1404–1410, 1987.

Tanaka, H., and M. D. Yamanaka, Atmospheric circulation in the lower stratosphere induced by the mesoscale mountain wave breakdown, *J. Meteorol. Soc. Jpn.*, *63*, 1047–1054, 1985.

Tsuda, T., T. Inoue, D. C. Fritts, T. E. VanZandt, S. Kato, T. Sato, and S. Fukao, MST radar observations of a saturated gravity wave spectrum, *J. Atmos. Sci.*, *46*, 2440–2447, 1989.

Tsuda, T., Y. Murayama, M. Yamamoto, S. Kato, and S. Fukao, Seasonal variation of momentum flux in the mesosphere observed with the MU radar, *Geophys. Res. Lett.*, *6*, 725–728, 1990.

Tsuda, T., T. E. VanZandt, M. Mizumoto, S. Kato, and S. Fukao, Spectral analysis of temperature and Brunt-Vaisala frequency fluctuations observed by radiosondes, *J. Geophys. Res.*, *96*, 17,265–17,278, 1991.

Tsuda, T., M. Nishida, C. Rocken, and R. H. Ware, A global morphology of gravity wave activity in the stratosphere revealed by the GPS occultation data (GPS/MET), *J. Geophys. Res.*, *105*, 7257–7273, 2000.

VanZandt, T. E., A universal spectrum of buoyancy waves in the atmosphere, *Geophys. Res. Lett.*, *9*, 575–578, 1982.

Vincent, R. A., Status of the SPARC Radiosonde Initiative, *SPARC Newsl.*, *20*, 17–18, 2003.

Vincent, R. A., and M. J. Alexander, Gravity waves in the tropical lower stratosphere: An observational study of seasonal and interannual variability, *J. Geophys. Res.*, *105*, 17,971–17,982, 2000.

Warner, C. D., and M. E. McIntyre, An ultrasimple spectral parameterization for nonorographic gravity waves, *J. Atmos. Sci.*, *58*, 1837–1857, 2001.

Yoshiki, M., and K. Sato, A statistical study of gravity waves in the polar regions based on operational radiosonde observation data, *J. Geophys. Res.*, *105*, 17,995–18,011, 2000.

S.-Y. Ogino, Graduate School of Science and Technology, Kobe University, Kobe 657-8501, Japan. (ogino@ahs.scitec.kobe-u.ac.jp)

K. Sato, Y. Tomikawa, and T. Yamanouchi, National Institute of Polar Research, Tokyo 173-8515, Japan. (kaoru@nipr.ac.jp; tomikawa@nipr.ac.jp; yamanouchi@pmg.nipr.ac.jp)

N. Takahashi, Department of Geophysics, Faculty of Science, Kyoto University, Kyoto 606-8502, Japan. (takahasi@kugi.kyoto-u.ac.jp)

M. Yamamori, Communications Research Laboratory, 4-2-1 Nukui-kitamachi, Koganei, Tokyo, Japan. (yamamori@crl.go.jp)